Subsonic to Supersonic Transition through a Vertical Pipe Bend

Etsuo Morishita

***Abstract*—**It is theoretically possible to accelerate the one-dimensional compressible pipe flow from subsonic to supersonic by the gravity effect through a vertical pipe bend. A viscous one-dimensional compressible pipe flow under gravity effect is first studied analytically. The compressible one-dimensional pipe flow with friction is called Fanno flow and the solution is given by analytical formula. In gas dynamics, the gravity effect is minimal and it is not included in the equations. However, it was shown by the present author that the elevation of a pipe could change the flow conditions in a one-dimensional compressible potential flow under gravity. The sonic condition is reached at the maximum height for an inviscid pipe flow. In this paper, the gravity effect is extended to the viscous one-dimensional pipe flow. Subsonic–supersonic transition is also possible by up and down of a pipe, i.e. through a vertical pipe bend for viscous flows, and it is found that the sonic condition deviates from the peak position of the pipe. The analytical solutions are obtained for the prescribed Mach number distribution. For the given pipe geometry, numerical approach is necessary, and the classical method of characteristics is applied to the problem and compared to the exact analytical solutions.

***Keywords*—**Aerodynamics, Compressible Flow, Pipe Bend, Gravity.

I. Introduction

In gas dynamics, the gravity effect is negligible and not included in the governing equations. However, the effect is evident in astrophysics, i.e. Bondi flow [1], [2]. It was also shown that an inviscid compressible one-dimensional pipe flow could be accelerated from subsonic to supersonic by the elevation of the pipe in theory [3]. Although the gravity effect is not evident in an ordinary air flow, it can be noticeable near the sonic condition and in the low acoustic velocity like cryogenics. This sonic condition occurs at the peak location of a pipe and the gravity has a similar effect to that of the throat of a Laval nozzle [3].

In order to apply this gravity effect in the real world problem, the viscous effect should be taken into account. A one-dimensional pipe flow with friction is called Fanno flow and the analytical solution is available [4], [5]. In the present analysis, the gravity term is added to the Fanno flow equations.

Etsuo Morishita is with the Mechanical Engineering Department, Meisei University, Tokyo, 191-8506, Japan (phone:+81(0)42-591-9612;e-mail: etsuo.morishita@meisei-u.ac.jp).

II. Governing Equations

A. Governing Equations

The continuity equation for a steady one-dimensional compressible pipe flow in Fig.1 is

$$\rho u = \rho^* u^* , \tag{1}$$

where u is the velocity, ρ is the density and the symbol * denotes the sonic condition. The momentum equation is given by

$$\rho u du + dp + \frac{4C_f}{D} \cdot \frac{1}{2} \rho u^2 \cdot dl + \rho g \cdot dz = 0 , \tag{2}$$

where C_f is the average skin friction coefficient, D is the pipe diameter, g is the gravitational acceleration, l is the coordinate along the pipe, p is the static pressure, x is the horizontal coordinate and z is the vertical coordinate.

The energy equation becomes

$$\frac{1}{2}u^2 + \frac{a^2}{\gamma - 1} + gz = \frac{1}{2}\frac{\gamma + 1}{\gamma - 1} a^{*2} + gz^* , \tag{3}$$

where a is the local acoustic velocity. Equation (3) is the Bernoulli's equation and the right hand side of (3) is constant.

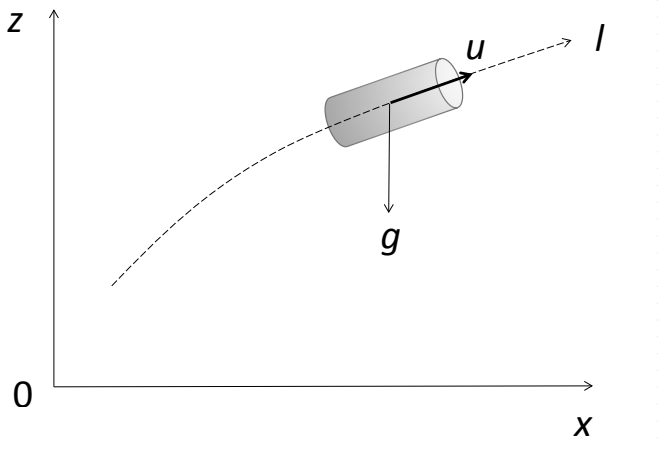

Fig. 1. Pipe coordinate system

The equation of state is given by

$$p = \rho RT \,. \tag{4}$$

From the definition of local Mach number M

$$M^2 = \frac{u^2}{a^2} = \frac{u^2}{\gamma RT}\,, \tag{5}$$

where R is the gas constant and γ is the specific heat ratio.

B. Modified Equations

Equations (1)-(5) are modified as follow:

$$\frac{d\rho}{\rho} + \frac{du}{u} = 0\,, \tag{6}$$

$$\gamma M^2 \frac{du}{u} + \frac{dp}{p} + \frac{4C_f}{D}\cdot\frac{1}{2}\gamma M^2 \cdot dl + \gamma\frac{gdz}{a^2} = 0\,, \tag{7}$$

$$(\gamma-1)M^2\frac{du}{u} + \frac{dT}{T} + (\gamma-1)\frac{gdz}{a^2} = 0\,, \tag{8}$$

$$\frac{dp}{p} = \frac{d\rho}{\rho} + \frac{dT}{T}\,, \tag{9}$$

$$\frac{dM^2}{M^2} = 2\frac{du}{u} - \frac{dT}{T}\,. \tag{10}$$

From (7) and (8) with (6), (9) and (10),

$$\left(M^2-1\right)\frac{du}{u} + \frac{4C_f}{D}\cdot\frac{1}{2}\gamma M^2\cdot dl + \frac{gdz}{a^2} = 0\,. \tag{11}$$

For an inviscid flow with $C_f = 0$,

$$\left(M^2-1\right)\frac{du}{u} + \frac{gdz}{a^2} = 0\,. \tag{12}$$

Equation (12) shows that $dz = 0$ at the sonic condition $M = 1$. This implies the sonic condition occurs at the pipe peak location $z = z^*$. For the viscous case at $M = 1$,

$$\frac{dz}{dl} = -\frac{4C_f}{D}\cdot\frac{1}{2}\gamma M^2\cdot\frac{a^2}{g}\,, \tag{13}$$

and the sonic condition is reaced after the pipe peak elevation.

From (6)-(10), the following relations are derived:

$$\frac{du}{u} = -\frac{d\rho}{\rho} = \frac{1}{2}\frac{1}{1+\frac{\gamma-1}{2}M^2}\frac{dM^2}{M^2} - \frac{\frac{\gamma-1}{2}}{1+\frac{\gamma-1}{2}M^2}\frac{gdz}{a^2}\,, \tag{14}$$

$$\frac{dp}{p} = -\frac{1}{2}\frac{1+(\gamma-1)M^2}{1+\frac{\gamma-1}{2}M^2}\frac{dM^2}{M^2} - \frac{\frac{\gamma-1}{2}}{1+\frac{\gamma-1}{2}M^2}\frac{gdz}{a^2}\,, \tag{15}$$

$$\frac{dT}{T} = -\frac{\frac{\gamma-1}{2}}{1+\frac{\gamma-1}{2}M^2}\frac{dM^2}{M^2} - \frac{\gamma-1}{1+\frac{\gamma-1}{2}M^2}\frac{gdz}{a^2}\,, \tag{16}$$

$$\frac{ds}{R} = \frac{\gamma}{\gamma-1}\frac{dT}{T} - \frac{dp}{p} = -\frac{dp_0}{p_0} = \frac{1}{2}\gamma M^2\cdot\frac{4C_f}{D}\cdot dl\,, \tag{17}$$

where p_0 is the local total pressure and s is the specific entropy. The local total pressure p_0 can be obtained from the local static pressure p by assuming isentropic compression. The first terms of the right hand side of (14)-(16) correspond to the Fanno flow solutions [4], [5], respectively.

C. Solution in Mach Numbers

From (8) and (10),

$$\frac{dM^2}{M^2} = 2\left(1+\frac{\gamma-1}{2}M^2\right)\frac{du}{u} + (\gamma-1)\frac{gdz}{a^2}\,. \tag{18}$$

From (11) and (18), the gravitational terms can be eliminated, and

$$\frac{du}{u} = -\frac{d\rho}{\rho} = \frac{4C_f}{D}\cdot\frac{1}{2}\frac{\gamma-1}{\gamma+1}\gamma M^2\cdot dl + \frac{1}{\gamma+1}\frac{dM^2}{M^2}\,. \tag{19}$$

Similarly,

$$\frac{dp}{p} = \frac{du}{u} - \frac{dM^2}{M^2} = \frac{4C_f}{D}\cdot\frac{1}{2}\frac{\gamma-1}{\gamma+1}\gamma M^2\cdot dl - \frac{\gamma}{\gamma+1}\frac{dM^2}{M^2}\,, \tag{20}$$

$$\frac{dT}{T} = 2\frac{du}{u} - \frac{dM^2}{M^2} = \frac{4C_f}{D}\frac{\gamma-1}{\gamma+1}\gamma M^2\cdot dl - \frac{\gamma-1}{\gamma+1}\frac{dM^2}{M^2}\,. \tag{21}$$

From (17), (19), (20), (21) and (3)

$$\ln\frac{u}{u^*} = 4C_f\cdot\frac{1}{2}\frac{\gamma(\gamma-1)}{\gamma+1}\cdot\int_{l^*/D}^{l/D} M^2\cdot d\left(\frac{l}{D}\right) + \frac{1}{\gamma+1}\ln M^2 \quad \left(=\ln\frac{\rho^*}{\rho}\right)\,, \tag{22}$$

$$\ln\frac{p}{p^*} = 4C_f\cdot\frac{1}{2}\frac{\gamma(\gamma-1)}{\gamma+1}\int_{l^*/D}^{l/D} M^2\cdot d\left(\frac{l}{D}\right) - \frac{\gamma}{\gamma+1}\ln M^2\,, \tag{23}$$

$$\ln\frac{T}{T^*} = 4C_f\cdot\frac{\gamma(\gamma-1)}{\gamma+1}\cdot\int_{l^*/D}^{l/D} M^2\cdot d\left(\frac{l}{D}\right) - \frac{\gamma-1}{\gamma+1}\ln M^2\,, \tag{24}$$

$$\frac{s-s^*}{R} = 4C_f\cdot\frac{\gamma}{2}\cdot\int_{l^*/D}^{l/D} M^2\cdot d\left(\frac{l}{D}\right), \tag{25}$$

$$\frac{g\left(z-z^*\right)}{a^{*2}} = \frac{1}{2}\frac{\gamma+1}{\gamma-1} - \frac{1}{2}\left(\frac{u}{u^*}\right)^2 - \frac{1}{\gamma-1}\frac{T}{T^*}\,, \tag{26}$$

where l^* is the pipe sonic point. Equations (22)-(26) do not necessarily give the flow solutions directly. However, the pipe vertical coordinate z relative to z^* can be calculated from (26)

with (22) and (24) when the Mach number distribution is assumed.

III. Mach Number Distribution

A. Inviscid Flow

In inviscid flows, the skin friction coefficient $C_f = 0$ and from (22) - (26) [3],

$$\frac{u}{u^*} = \frac{\rho^*}{\rho} = M^{\frac{2}{\gamma+1}}, \tag{27}$$

$$\frac{p}{p^*} = M^{\frac{2\gamma}{\gamma+1}}, \tag{28}$$

$$\frac{T}{T^*} = \frac{1}{M^{2\frac{\gamma-1}{\gamma+1}}}, \tag{29}$$

$$\frac{s-s^*}{R} = 0 \ , \tag{30}$$

$$\frac{z-z^*}{\left(\frac{a^{*2}}{g}\right)} = \frac{1}{2}\frac{\gamma+1}{\gamma-1} - \frac{1}{2}M^{\frac{4}{\gamma+1}} - \frac{1}{\gamma-1}\frac{1}{M^{2\frac{\gamma-1}{\gamma+1}}}. \tag{31}$$

In this case, Mach number M can be calculated for a given $\left(z-z^*\right)/\left(a^{*2}/g\right)$ from (31).

Figure 2 shows the Mach number distribution for $\gamma = 1.4$ and

$$\frac{z-z^*}{\left(\frac{a^{*2}}{g}\right)} = -1 + \exp\left[-3\left(\frac{x}{D}\right)^2\right].$$

The elevation of pipe position has the same effect as that of the cross section of a Laval nozzle. The sonic condition occurs at the peak height of the pipe.

B. Viscous Flow Acceleration

The viscous flow solutions (22) - (26) are effective when the Mach number distribution is assumed. For example, a simple distribution from subsonic to supersonic transition can be given as follows:

$$M^2 = 1 + \frac{l}{D} \quad \left(\frac{l}{D} > -1\right),$$

where

$$\frac{l^*}{D} = 0 \quad (M = 1).$$

The integral in (22) - (25) becomes

$$\int_{l^*/D}^{l/D} M^2 \cdot d\left(\frac{l}{D}\right) = \left(\frac{l}{D}\right) + \frac{1}{2}\left(\frac{l}{D}\right)^2.$$

Then, (22) - (26) become explicit function of l/D and the pipe elevation (26) is obtained inversely.

Figure 3 shows the pipe geometry for the given Mach number distribution with skin friction coefficients as parameters.

As mentioned in (13) the subsonic-supersonic transition occurs at $l/D = l^*/D = 0$ after the peak elevation of the pipe for $C_f > 0$, while the inviscid flow reaches the sonic condition at the peak elevation of the pipe. It means that the flow has to be accelerated by gravity to overcome the pipe friction to be supersonic.

From (11), it is clear that the following equation is satisfied at the pipe peak position $dz = 0$:

$$\left(M^2 - 1\right)\frac{du}{u} + \frac{4C_f}{D} \cdot \frac{1}{2}\gamma M^2 \cdot dl = 0 \ . \tag{32}$$

From Fig.3, the peak location of the pipe moves upstream as the skin friction coefficient C_f increases.

Figure 4 shows the flow properties for $C_f = 0.05$ in Fig.3. The temperature ratio T/T^* rises gradually $l/D > 0.9$ for $C_f = 0.05$, while it decreases monotonically for the inviscid flow.

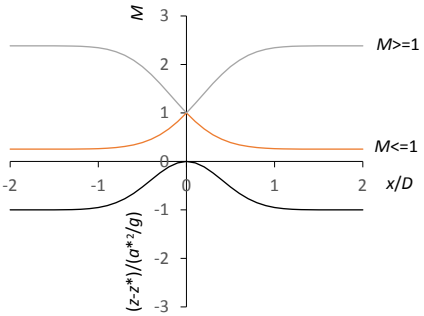

Fig. 2. Mach number distribution of inviscid pipe flow γ=1.4

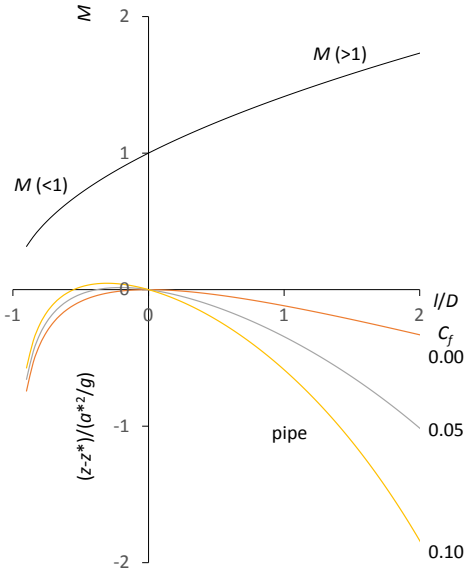

Fig. 3. Pipe geometry for $M = \sqrt{1 + \left(l/D\right)}$ and $\gamma = 1.4$

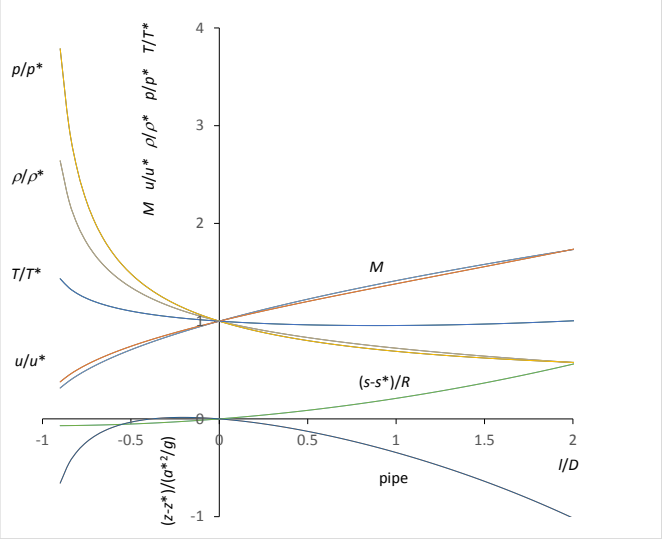

Fig. 4. Flow properties for $C_f = 0.05$ in Fig.2

C. Viscous Flow Deceleration

Flow deceleration is also studied analytically. The Mach number might be assumed as

$$M^2 = 1 - \frac{l}{D} \quad \left(\frac{l}{D} < 1\right).$$

The integral in (22) - (25) becomes

$$\int_{l^*/D}^{l/D} M^2 \cdot d\left(\frac{l}{D}\right) = \left(\frac{l}{D}\right) - \frac{1}{2}\left(\frac{l}{D}\right)^2.$$

Equations (22) - (26) become explicit function of l/D and the pipe elevation (26) is obtained inversely as before.

Figure 5 shows the pipe geometry as a function of l/D for the given Mach number distribution with the several different values of C_f. The deceleration of supersonic flow requires an ascent for small values of C_f, while a continuous descent is necessary to decelerate the flow for large values of C_f. This behaviour can be explained from (11). From (11),

$$\frac{gdz}{a^2} = -\left(M^2 - 1\right)\frac{du}{u} - \frac{4C_f}{D} \cdot \frac{1}{2}\gamma M^2 \cdot dl. \qquad (33)$$

Equation (33) can be negative for large values of C_f even for decelerating supersonic flow $(du < 0, M > 1)$.

Flow properties are shown in Fig.6 for $C_f = 0.05$ in Fig 5.

IV. Numerical Analysis

Numerical method is required to determine the flow properties for a given pipe geometry. The classical method of

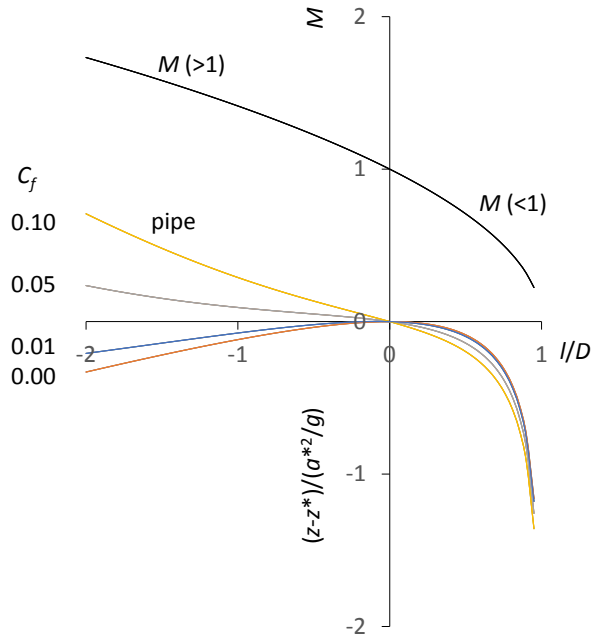

Fig. 5. Pipe geometry for $M = \sqrt{1-(l/D)}$ and $\gamma = 1.4$

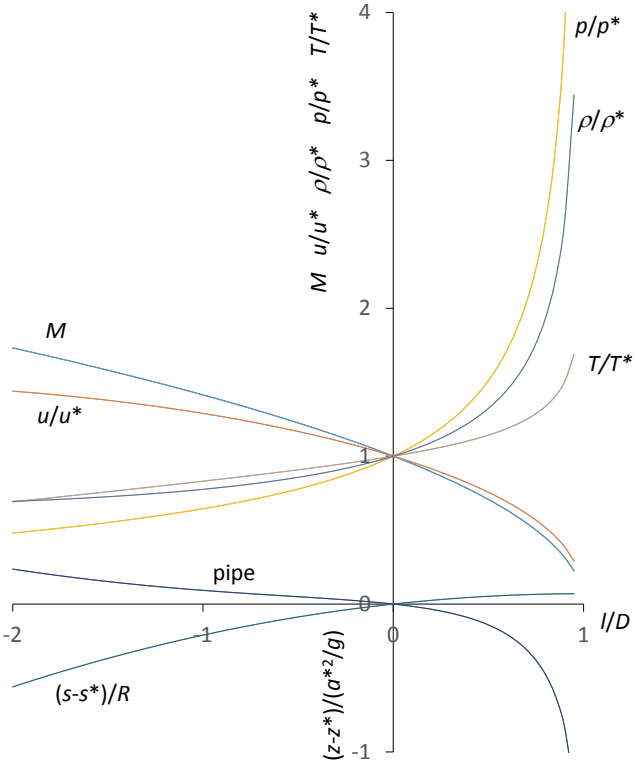

Fig. 6. Flow properties for $C_f = 0.05$ in Fig.3

characteristics is applied to the governing equations. The continuity, the momentum, and the energy equations are:

$$\frac{\partial}{\partial t}\rho + \frac{\partial}{\partial l}(\rho u) = 0, \qquad (34)$$

$$\rho\frac{\partial u}{\partial t}+\rho u\frac{\partial u}{\partial l}=-\frac{\partial p}{\partial l}-\frac{1}{2}\rho u^2\cdot\frac{4C_f}{D}-\rho g\frac{\partial z}{\partial l}, \tag{35}$$

$$\frac{\partial \rho e_t}{\partial t}+\frac{\partial}{\partial l}\left(\rho u e_t+\rho g z u+pu\right)=0, \tag{36}$$

where e_t is the specific total energy,

$$e_t\equiv e+\frac{u^2}{2}, \tag{37}$$

e is the specific internal energy, and t is the time.

From (34) - (37),

$$\frac{1}{\rho a}\frac{\partial p}{\partial t}+a\frac{\partial u}{\partial l}+\frac{u}{\rho a}\frac{\partial p}{\partial l}=0, \tag{38}$$

$$\frac{\partial u}{\partial t}+u\frac{\partial u}{\partial l}+\frac{a}{\rho a}\frac{\partial p}{\partial l}=-\frac{1}{2}u^2\cdot\frac{4C_f}{D}-g\frac{\partial z}{\partial l}. \tag{39}$$

The sum and the subtraction of (38) and (39) become respectively

$$\begin{aligned}&\frac{\partial u}{\partial t}+\left(u+a\right)\frac{\partial u}{\partial l}+\frac{1}{\rho a}\left[\frac{\partial p}{\partial t}+\left(u+a\right)\frac{\partial p}{\partial l}\right],\\&=-\frac{1}{2}u^2\cdot\frac{4C_f}{D}-g\frac{\partial z}{\partial l}\end{aligned} \tag{40}$$

$$\begin{aligned}&\frac{\partial u}{\partial t}+\left(u-a\right)\frac{\partial u}{\partial l}-\frac{1}{\rho a}\left[\frac{\partial p}{\partial t}+\left(u-a\right)\frac{\partial p}{\partial l}\right].\\&=-\frac{1}{2}u^2\cdot\frac{4C_f}{D}-g\frac{\partial z}{\partial l}\end{aligned} \tag{41}$$

Along the two characteristic lines C^+ and C^-,

$$d\left(u+\frac{p}{\rho a}\right)=f\cdot\Delta t\qquad C^+:\frac{dl}{dl}=u+a, \tag{42}$$

$$d\left(u-\frac{p}{\rho a}\right)=f\cdot\Delta t\qquad C^-:\frac{dl}{dt}=u-a, \tag{43}$$

where

$$f\equiv-\frac{1}{2}u^2\cdot\frac{4C_f}{D}-g\frac{\partial z}{\partial l}. \tag{44}$$

Equations (42) and (43) are integrated along the characteristic lines respectively as follow:

$$u_C+\frac{2a_C}{\gamma-1}=u_A+\frac{2a_A}{\gamma-1}+f_A\cdot\Delta t, \tag{45}$$

$$u_C-\frac{2a_C}{\gamma-1}=u_B-\frac{2a_B}{\gamma-1}+f_B\cdot\Delta t, \tag{46}$$

where the suffix A denotes a point on the C^+ characteristic line at t, the suffix B denotes a point on the C^- characteristic line at t, and the suffix C represents the cross point of the two characteristic lines at $t+\Delta t$. Equations (45) and (46) give the solutions as follow:

$$u_C=\frac{u_A+u_B}{2}+\frac{1}{\gamma-1}\left(a_A-a_B\right)+\frac{f_A+f_B}{2}\Delta t, \tag{47}$$

$$a_C=\frac{\gamma-1}{4}\left(u_A-u_B\right)+\frac{a_A+a_B}{2}-\frac{\gamma-1}{4}\left(f_A-f_B\right)\Delta t. \tag{48}$$

One of the boundary conditions becomes

$$u_C=u_B-\frac{2}{\gamma-1}\left(a_B-a_C\right)+f_B\cdot\Delta t, \tag{49}$$

when the inlet subsonic a_C is given. The supersonic outlet condition is automatically calculated from the upstream values.

The linear interpolation is applied for constant Δl as follows [6]. Along the C^+ characteristics,

$$u_A=u_{i-1}+\frac{\Delta l-\left(u+a\right)\Delta t}{\Delta l}\left(u_i-u_{i-1}\right), \tag{50}$$

$$a_A=a_{i-1}+\frac{\Delta l-\left(u+a\right)\Delta t}{\Delta l}\left(a_i-a_{i-1}\right), \tag{51}$$

$$f_A=f_{i-1}+\frac{\Delta l-\left(u+a\right)\Delta t}{\Delta l}\left(f_i-f_{i-1}\right). \tag{52}$$

Along the C^- characteristics for subsonic flow,

$$u_B=u_i+\frac{-\left(u-a\right)\Delta t}{\Delta l}\left(u_{i+1}-u_i\right), \tag{53}$$

$$a_B=a_i+\frac{-\left(u-a\right)\Delta t}{\Delta l}\left(a_{i+1}-a_i\right), \tag{54}$$

$$f_B=f_i+\frac{-\left(u-a\right)\Delta t}{\Delta l}\left(f_{i+1}-f_i\right). \tag{55}$$

For supersonic flow,

$$u_B=u_{i-1}+\frac{\Delta l-\left(u-a\right)\Delta t}{\Delta l}\left(u_i-u_{i-1}\right), \tag{56}$$

$$a_B=a_{i-1}+\frac{\Delta l-\left(u-a\right)\Delta t}{\Delta l}\left(a_i-a_{i-1}\right), \tag{57}$$

$$f_B=f_{i-1}+\frac{\Delta l-\left(u-a\right)\Delta t}{\Delta l}\left(f_i-f_{i-1}\right), \tag{58}$$

where i denotes the node which is equally spaced Δl.

Figures 7 (a), (b) and (c) show the comparison between the method of characteristics and the analytical results. Note that the numerical method first gives the pipe geometry, while the analytical solutions are devised to obtain the pipe geometry for the given Mach number, see Fig.3. The difference between the analytical solutions and the numerical method becomes noticeable at larger friction coefficients.

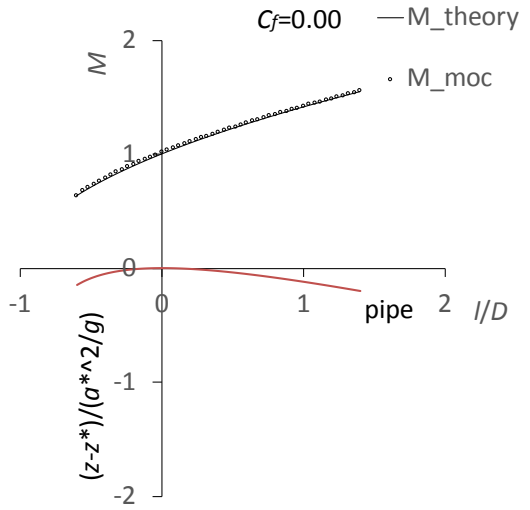

(a)

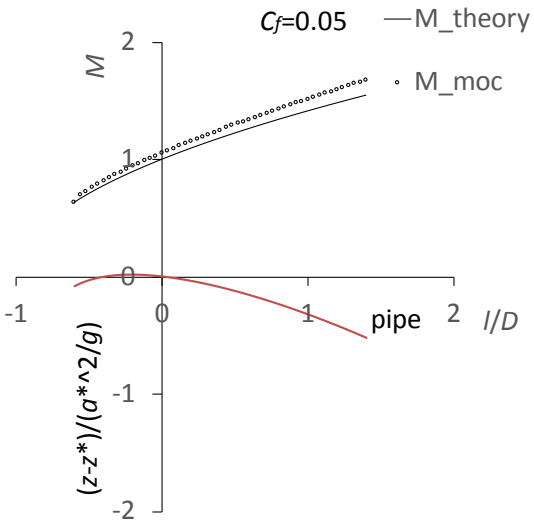

(b)

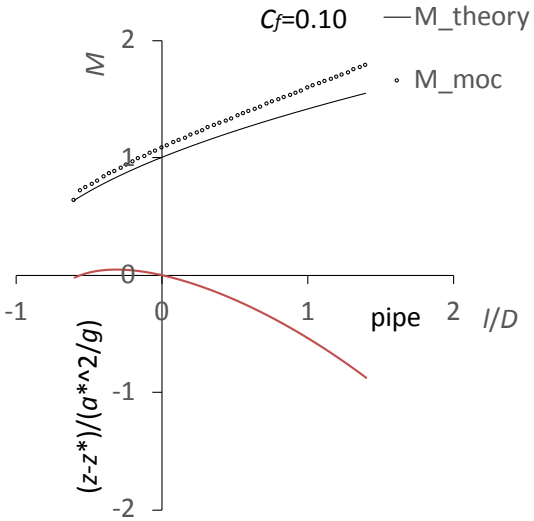

(c)

Fig. 7. Mach number distribution by method of characteristics

V. Engineering Application

Subsonic-supersonic transition in a constant sectional area pipe by gravity effect is important from an engineering point of view.

Figure 8 shows an inviscid pipe flow with $g = 9.8\text{m/s}^2$ and $a^* = 100\text{m/s}$ derived from Fig. 2. Therefore, the subsonic flow can be accelerated to a supersonic one with up and down of about 10m around the peak of the pipe. The Mach number solely depends the height of the pipe $z - z^*$.

For $g = 9.8\text{m/s}^2$ and $a^* = 100\text{m/s}$, a subsonic flow of $M \approx 0.25$ can be accelerated to a supersonic flow of $M \approx 2.4$ by $z - z^* \approx 1000\text{m}$ in Fig.2. The scale of the height is that of an planetary flow [7].

As for the viscous pipe flow solutions, the Mach number distribution is assumed along the pipe length l. From Fig.1, geometric relations is

$$\Delta l^2 = \Delta x^2 + \Delta z^2 .$$

Therefore, the following conditions must be satisfied to obtain the physically proper solution:

$$-1 \le \frac{dz}{dl} = \frac{\left(\frac{a^{*2}}{g}\right)}{D} \frac{d\left[\frac{(z-z^*)}{\left(\frac{a^{*2}}{g}\right)}\right]}{d\left(\frac{l}{D}\right)} \le 1 . \tag{59}$$

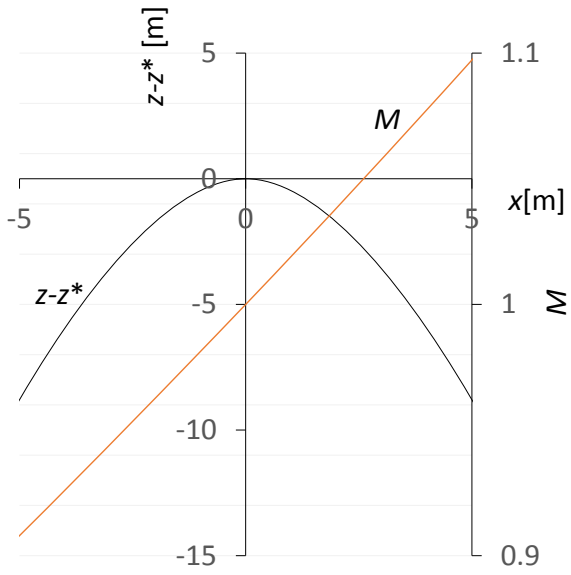

Fig. 8. Inviscid pipe flow subsonic-supersonic transition by gravity $g = 9.8\text{m/s}^2$ and $a^* = 100\text{m/s}$

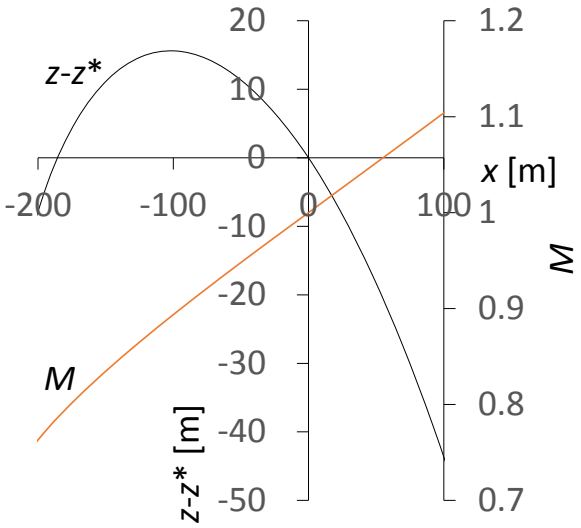

Fig. 9. Viscous pipe flow subsonic-supersonic transition by gravity $g = 9.8\text{m/s}^2$, $a^* = 100\text{m/s}$, $C_f = 0.05$ and $D = 500\text{m}$ in Fig.3

Figure 9 shows an example of the viscous pipe flow with gravity derived from Fig.3, where the pipe diameter is given as $D = 500\,\text{m}$ to fit the geometric condition $|dz/dl| \le 1$ with $g = 9.8\text{m/s}^2$, $a^* = 100\text{m/s}$, and $C_f = 0.05$, although D is not a realistic value as an engineering problem. However, it might be possible for a planetary flow [7].

Note that lateral coordinate is transformed to x from l measured along the pipe in Fig.9.

VI. Concluding Remarks

Compressible pipe flow with friction and gravity is modelled analytically. The viscous pipe flow is known as Fanno flow and choke occurs at the exit of the pipe. To accelerate a flow from subsonic to supersonic by gravity is theoretically possible for an inviscid pipe flow as previously shown by the present author. The subsonic-supersonic transition is also possible for the viscous pipe flow with gravity. The sonic condition is reached after the pipe peak elevation in this case. For deceleration from a supersonic flow to a subsonic one, there is no peak for larger pipe frictions, while an inviscid supersonic flow goes upwards to decelerate to the sonic condition and downwards for subsonic deceleration.

For a given pipe geometry, the method of characteristics is applied. The numerical results are compared to those of the exact analytical solutions, and the greater the friction, the greater the difference although the numerical results are satisfactory in the practical implications.

The subsonic-supersonic transition might be possible by up and down of a pipe for both inviscid and viscous flows in theory. Although it is not an easy task to achieve this condition in a laboratory scale, it could be possible in cryogenics, planetary and astrophysics conditions.

References

[1] H. Bondi, H., Mon. Not. R. Astron. Soc. 112, 95 (1952)
[2] S. N. Shore, An Introduction to Astrophysical Hydrodynamics (Academic Press, San Diego, 1992)
[3] E. Morishita, Proc. WEC Vol III, London (2013) Available: http://www.iaeng.org/publication/WCE2013/WCE2013_pp1739-1742.
[4] M. A. Saad, Compressible Fluid Flow (Prentice-Hall, Englewood Cliffs, 1993)
[5] J. D. Anderson, Modern Compressible Flow: With Historical Perspective (McGraw-Hill, New York, 2004)
[6] C.Y. Chow, An Introduction to Computational Fluid Mechanics (John Wiley & Sons, Hoboken, 1979)
[7] Sharghi, K., Supersonic Wind, Available: https://nasaviz.gsfc.nasa.gov/11349 (2013)